Decay of first-year sea ice

Johnston, Michelle; Frederking, Robert; Timco, Garry

Publisher's version / Version de l'éditeur:
https://doi.org/10.4224/12326980
Technical Report (National Research Council Canada. Canadian Hydraulics Centre); no. HYD-TR-058, 2001-04

CHC CANADIAN HYDRAULICS CENTRE
CENTRE D'HYDRAULIQUE CANADIEN

TP 13940E

SEASONAL DECAY OF FIRST-YEAR SEA ICE

M. Johnston, R. Frederking and G. Timco

Technical Report HYD-TR-058

April 2001

National Research Council Canada
Conseil national de recherches Canada

CHC CANADIAN HYDRAULICS CENTRE

SEASONAL DECAY OF FIRST-YEAR SEA ICE

Final Report
submitted to:

Robert L. Wolfe
Research and Development Officer
Transport Canada, Prairie and Northern Marine
Tower C, Place de Ville
14th Floor, 330 Sparks Street
Ottawa, Ontario K1A 0R6

and

Roger De Abreu
Environment Canada, Remote Sensing and Modelling
Canadian Ice Service
373 LaSalle Academy
Ottawa, Ontario K1A 0E6

Prepared By:

M. Johnston, R. Frederking and G. Timco
Canadian Hydraulics Centre
National Research Council of Canada
Building M-32, Montreal Road
Ottawa, Ontario K1A 0R6

Technical Report HYD-TR-058

April 2001

Abstract

This report describes analysis results of one season of measurements of decayed first year sea ice in the central Canadian Arctic. The study was conducted from 21 May to 19 July 2000. Mean air temperatures steadily increased from –15°C to a maximum of +7.5°C. The ice was 1.20 m thick on 21 May and had ablated to 0.83 m by 19 July. Ice ablation occurred at a rate of about 23 mm/day. The initial bulk ice salinity of 5.5 ‰ had decreased to less than 0.5 ‰ by 19 July. The upper and lower surfaces of the ice began to desalinate before the bulk layer of ice. The confined compressive strength of the ice was measured in 110 borehole jack tests. All strength profiles showed that the *in situ* ice strength decreased as the decay season progressed. Over the nine-week period, the average full-thickness *in situ* strength of the ice decreased from 12 MPa to 3 MPa. Most of the decrease in *in situ* ice strength resulted from changes in the physical properties of the ice. During the last three weeks of the study, the ice maintained a strength of 3 MPa whereas ice ablation continued until the end of the study.

Table of Contents

List of Figures

SEASONAL DECAY OF FIRST-YEAR SEA ICE

1. Introduction

Previously, ice property measurements have been conducted before mid-May (Sinha, 1986; Prowse et al., 1988; Sinha, 1990; and Masterson et al., 1997). Early in the spring season, site access presents little logistical trouble and measurement techniques are relatively straightforward. Once air temperatures warm and solar radiation increases, the snow and ice rapidly begin to melt. Morphological changes in the ice occur shortly after a core is removed from the ice sheet, which makes field measurements exceedingly difficult. Studies that have been conducted during melt onset have focused upon the snow and ice surface (Barber, 1997); measurements that do not require ice core extraction. Those studies focussed upon the ice surface layer because of its primary importance to the remotely sensed imagery that is used to characterize ice conditions by, for example, Canadian Ice Service (CIS) and the United States National Ice Centre (NIC).

The limited amount of data on the decay of first year sea ice lead to the development of a field program that would provide physical property measurements of the ice surface and the bulk layer of ice during decay. The program was developed by Canadian Hydraulics Centre (CHC). Canadian Ice Service (CIS) performed the required measurements. The field project was conducted under the auspices of the Collaborative-Interdisciplinary Cryospheric Experiment (C-ICE'00) of the University of Manitoba. Polar Continental Shelf Project (PCSP) provided field support.

This report presents an analysis of data acquired over a nine-week field program that extended from 21 May to 19 July 2000. The analysis was based upon physical property measurements of the snow and ice. The *in situ* confined compressive strength of the ice was measured using a borehole jack assembly. The reader is referred to Johnston and Frederking (2000) for details of the field program.

2. Measurements Performed during the Field Work

The present field program was conducted from melt onset (early May) to the later stages of ice decay (mid-July). The property measurements were classified according to surface properties and ice properties in the bulk layer of ice (Figure 1). Measured surface properties included the snow depth (d_s), snow density (r_s) and air temperature (t_a). Bulk ice properties included the ice freeboard (f_i), ice thickness (d_i), ice temperature (t_i), ice salinity (s_i) and the *in situ* compressive strength (borehole strength, s_i) of the ice.

The *in situ* borehole strength of the ice (s_i) was related to the flexural (s_f) and compressive (s_c) strengths of the ice that are commonly calculated from the equations developed by Timco and O'Brien (1994) and Timco and Frederking (1990) respectively. The environmental parameters required in the strength calculations include the ice density (r_i), brine volume (n_b) and/or total ice porosity (n_t, sum of brine volume and air porosity).

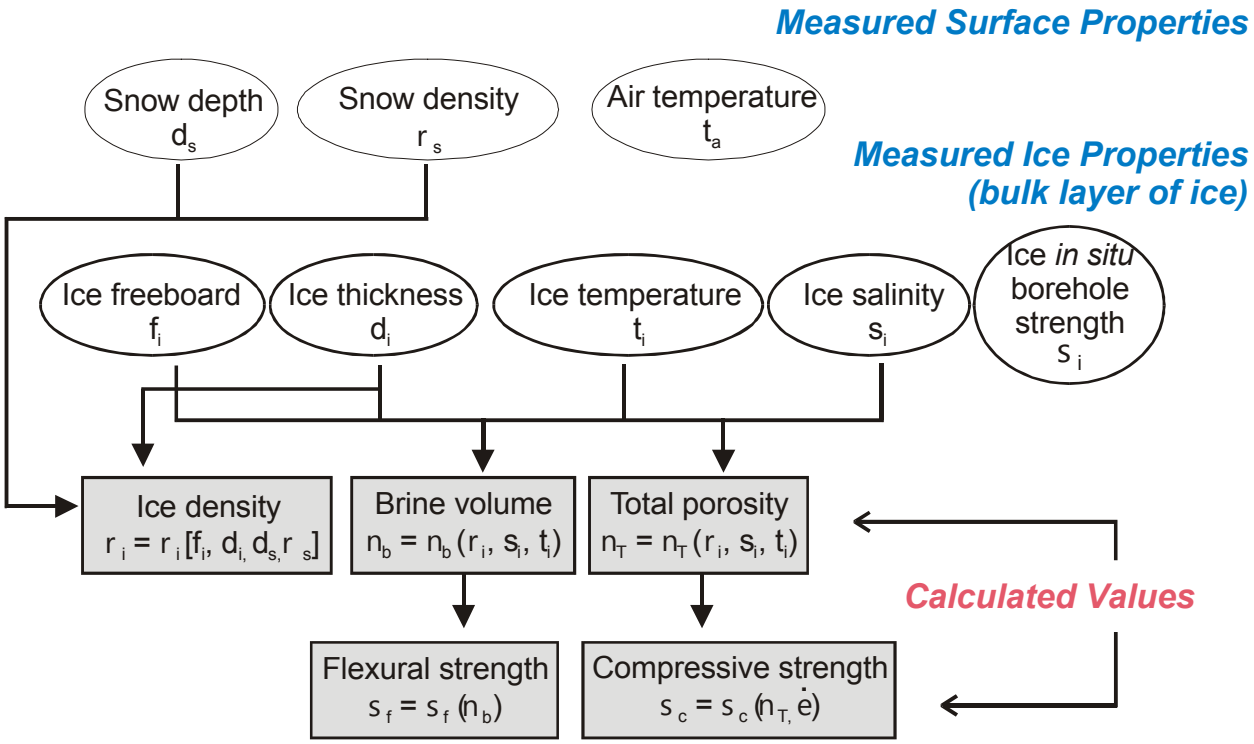

[ ] was used to include the properties used to calculate the parameter as opposed to
( ) which indicates that the parameter is a function of those properties

Figure 1 Parameters used to characterize ice decay

3. Methodology for Field Measurements

The Collaborative-Interdisciplinary Cryospheric Experiment (C-ICE'00) base camp was located on Truro Island, west of Cornwallis Island, Nunavut. The measurement site was selected as landfast ice in McDougall Sound, 5 km east of camp. The ice was sufficiently level, had a moderately thick snow cover (0.18 m in early May) and no evidence of roughness or pressure ridging (Figure 2).

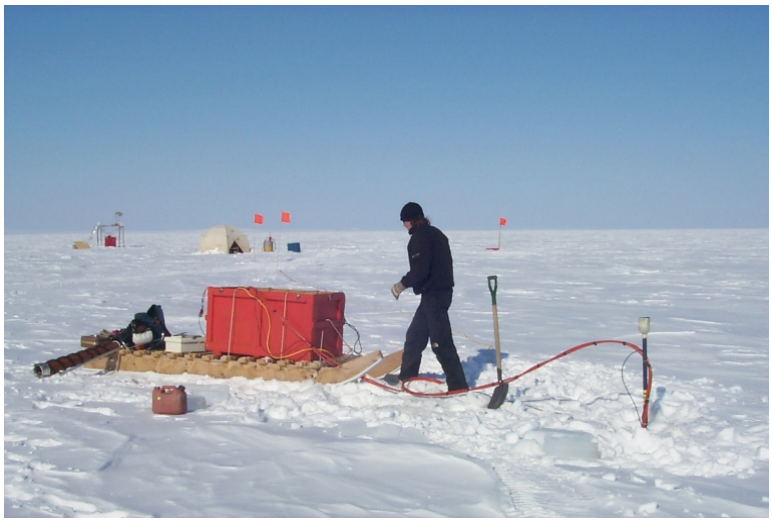

Figure 2 Measurement site on first year ice in McDougall Sound (photo taken in late May, courtesy of K. Wilson)

Following is a brief description of the methodology used to measure the physical properties listed in Figure 1 during the decayed ice study. The reader is referred to Johnston and Frederking (2000) for a more detailed description of the measurement program.

The program extended from 21 May to 19 July 2000. Snow and ice property measurements were conducted over a 900 m² area of ice from 21 May to 1 July. Each week, a field party visited the same area of ice by snowmobile and performed the requested measurements at stations selected about 5 m apart. As the decay season advanced, site visits were made twice per week.

A motor driven, fibre glass corer was used to make a triangular pattern of 150 mm diameter, smooth walled, vertical boreholes in the ice. The boreholes were about 1.5 to 2.0 m apart. The ice thickness, freeboard and snow depths at each borehole were measured. An ice core from one of the boreholes was used to measure the ice temperature by inserting a thermal probe into small holes made in the core at depth intervals of 0.15 m. The ice core from the second borehole was sectioned into 20 mm

discs (at 0.15 m depth intervals). The discs of ice were then melted and a calibrated conductivity meter was used to measure the salinity of the melt-water. The cores were sectioned as quickly as possible to minimize brine drainage. The core from the third borehole was not used for property measurements.

The ice *in situ* borehole strength (or *in situ* compressive strength) was measured at each of the three holes using a borehole jack assembly. The borehole jack consists of a high-strength stainless steel hydraulic cylinder with a laterally acting piston and two indentor plates, curved to match the wall of the borehole (Figure 3). Once activated, the piston inside the body of the jack applies hydraulic pressure to the front and back indentor plates. The oil pressure and displacement of the indentor plate are recorded by an external digital acquisition system (see Frederking, 2000 for details).

Borehole jack tests for each hole were conducted at depth intervals of 0.30 m. Typically, four borehole jack tests were performed at each hole before the bottom of the ice was reached. During the tests, the indentor plate was extended continuously until the limit of the stroke ram was reached (25 mm total diametrical displacement) or concern was expressed about overloading the jack. At that point the indentor plates were retracted fully, the jack was rotated 90° and lowered to the next test depth.

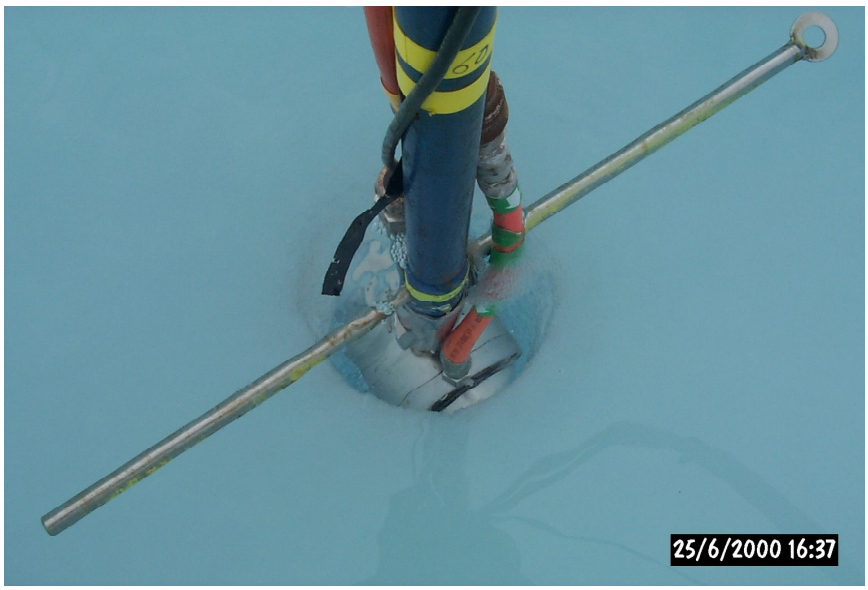

Figure 3 Borehole jack indentor
(courtesy of D. Bradley)

4. Physical Property Measurements

Ten site visits were conducted during the nine-week field program. Nine of those visits were made while the C-ICE camp on Truro Island was still in operation. By 1 July it was no longer safe to travel on the ice by snowmobile and the C-ICE camp was decommissioned. Two weeks later, on 19 July, personnel from Canadian Ice Service made the tenth and final visit to the site using the CCGS Louis S. St. Laurent to access decayed ice at the main site. Ice in the vicinity of the main site broke up on 28 July, eleven days after the last measurements were taken (DeAbreu, personal communication). Break-up was caused by the southward migration of a polyna along the east shore of McDougall Sound.

Three other sites were also visited with the Louis S. St. Laurent on 19 and 20 July. On the afternoon of 19 July, the vessel stopped in central McDougall Sound to sample what was surprisingly thick first-year sea ice. The ice thickness at that site ranged from 1.5 m to more than 2.1 m (limit of the ice auger). On 20 July two additional sites were sampled in Barrow Strait. The ice thickness at those sites ranged from 0.30 to 1.15 m.

The ice sites sampled during this program provide quantitative data about the most advanced stages of ice decay measured to date. Ice property measurements from the main site provide a continuous record of the decay process in the same area of ice, hence they form the basis of this report. Measurements from the additional sites sampled on 19 and 20 July are mentioned briefly, since a continuous record was not available for those sites.

4.1 Surface Characteristics Associated with the Decay Process

As the decay season progressed, the ice began to develop an undulating surface. Melt ponds covered some areas of ice, while other regions began to develop a hummocked appearance (elevated, white, porous ice, Figure 4). Since it became exceedingly difficult to locate level ice, measurements were taken in ponded ice and hummocked ice as a matter of course. The following discussion was based upon the average properties measured at each station (two to four boreholes) at the main ice site.

Figure 4 Late season surface topography of decayed first-year ice (21 July, courtesy of D. Bradley)

4.2 Air Temperature and Ice Temperature

Figure 5 shows the mean air temperature (courtesy of Atmospheric Environment Service). The air temperature was –15°C when the ice site was first visited on 21 May (JD142). On 10 June (JD162) the mean air temperature rose above zero for the first time that season. Subsequent air temperatures remained above zero and continued to increase, with occasional, brief cooling trends. The maximum air temperature during the sampling period was +7.5°C on 7 July (JD189).

The surface temperatures of the ice shown in Figure 5 were obtained by inserting the thermal probe into the extracted ice cores. Ice temperatures were also obtained from two strings of thermocouples frozen into the ice by University of Manitoba personnel. Temperatures measured from the extracted ice core agreed favorably with measurements from one of the string of thermocouples[1] early in the season. After JD163, temperature measurements from the extracted ice cores became less reliable, as shown in Figure 5. Unfortunately, no ice temperatures were available from the string of thermocouples, since it had melted from the ice at that point.

[1] The first string of thermocouples (first dowel) produced erratic temperature data. Therefore, ice core temperatures were compared with thermocouple measurements from the second dowel (installed below 0.60 m).

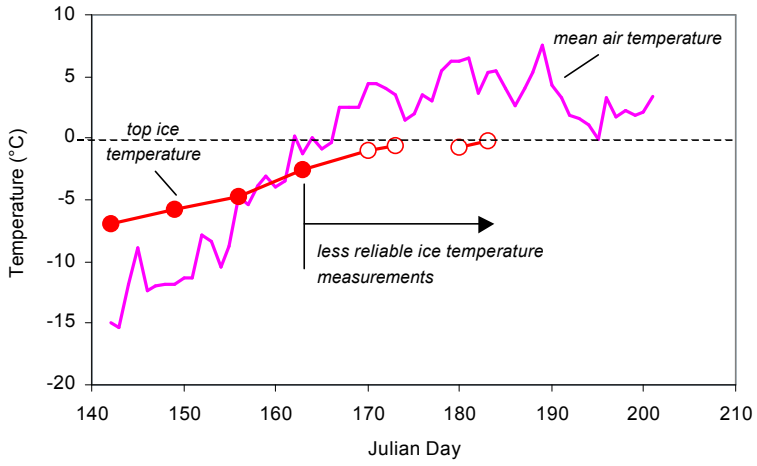

Figure 5 Air temperatures and top ice temperatures during study

4.3 Snow and Ice Thickness

Figure 6 shows measurements of the snow and ice thickness during the study. During the first week, air temperatures remained cold and the 0.18 m thick snow cover melted little. On 4 June (JD156) both the snow cover and ice thickness had reached a maximum (0.27 m, and 1.55 m respectively). By 18 June (JD170), increasing air temperatures caused the 270 mm snow cover to rapidly decrease to just 40 mm. Results show that the first decrease in ice thickness occurred on 18 June (JD170) indicating that, once the ice surface was exposed, the ice began to ablate. After 18 June, ice ablation continued until the end of the study, at relatively constant rate of 23 mm per day. By the end of the study ice thickness had decreased to 0.83 m (19 July, JD201).

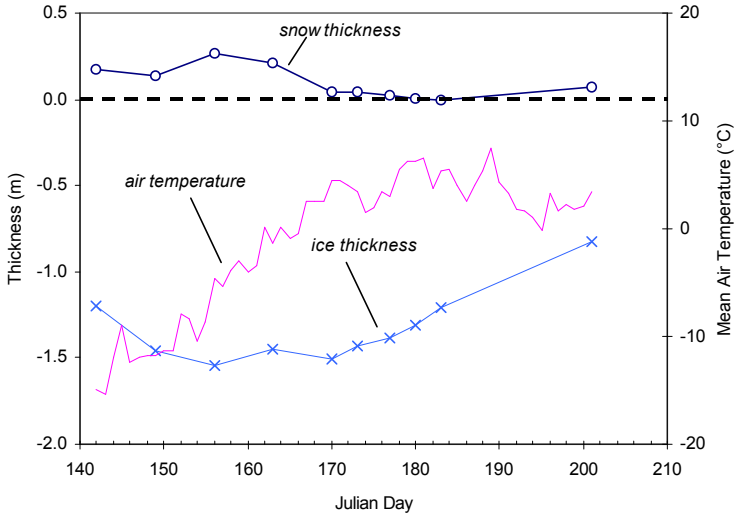

Figure 6 Snow and ice thickness during the study

4.4 Ice Freeboard

Figure 7 shows the variation in ice freeboard measured at the individual boreholes on each test day. There was significant variation in freeboard measurements made during the field program. The variation is not surprising considering that, as the melt season progressed, some areas of the ice were submerged beneath melt ponds while other areas of the ice surface were elevated. Two of the borehole jack tests were actually conducted in ponded ice, as shown by their negative freeboard (JD177 and JD201).

Initially, it was envisioned that a bulk ice density could be estimated using the measured ice freeboard, snow/ice thickness and snow density. The range of densities obtained using that approach (0.91 to 1.01 Mg/m³) showed that it was not feasible to estimate ice density from freeboard estimates. In order for freeboard measurements to provide valid ice densities, the ice would need to be independent of boundary effects imposed by the surrounding ice. That would require cutting a full-thickness block of ice from the sheet and measuring the its freeboard while floating in position; a procedure that involves considerable time and effort.

Timco and Frederking (1996) provide a review of the different techniques that can be used to measure the ice density. The authors compiled the ice densities reported in the literature and found significant variation in the reported ice density measurements of first year sea ice (0.84 to 0.94 Mg/m³). That variation was attributed to measurement techniques and improper handling of the ice after it was removed from the ice sheet. As yet, there is no simple methodology that can be used to obtain accurate ice density measurements; particularly ice that is within several degrees of its melting point.

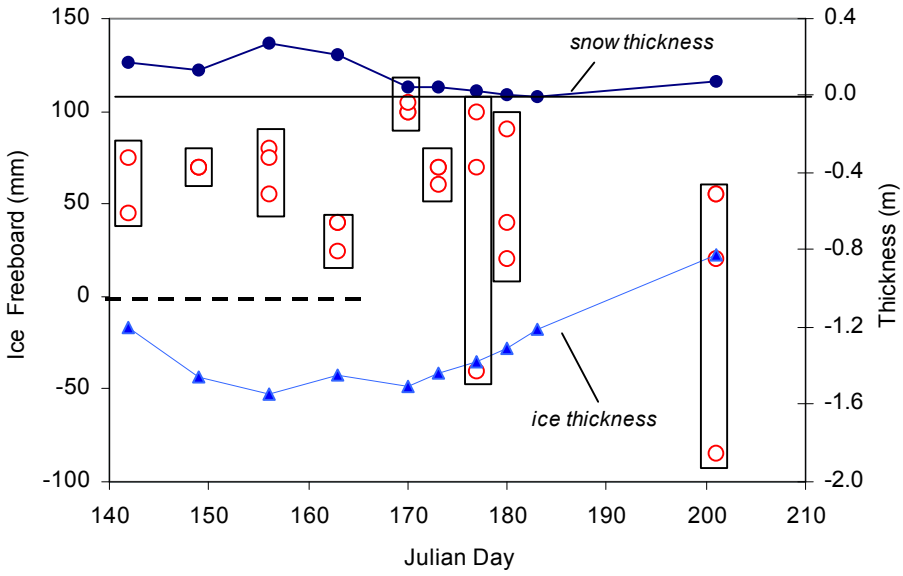

Figure 7 Variation in ice freeboard at individual boreholes

4.5 Ice Salinity

Figure 8 shows the salinity profiles that were measured from one of the ice cores for each sampling date. The ice salinity profiles remained relatively stable until 18 June (JD170), excepting the decrease in the ice surface salinity between JD142 and JD149 (believed to be inaccurate). The ice salinity profiles began to change after 18 June (JD170). The surface salinity decreased by 6‰ and there was a 1‰ decrease in salinity at the bottom of the ice. Recall that it was on 18 June that the ice first began to decrease in thickness. On 19 July (JD201) the ice had a salinity of less than 0.5 ‰ throughout its full thickness of 0.83 m.

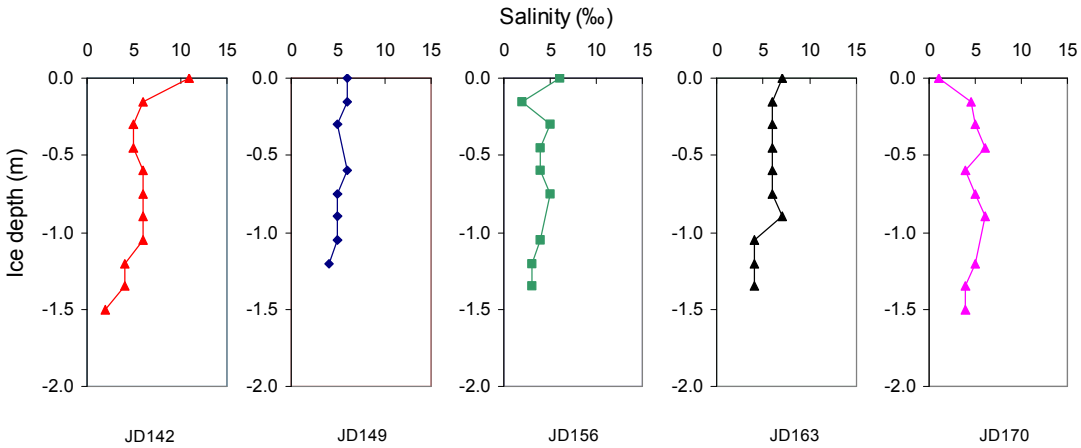

(a) 21 May (JD142) to 18 June (JD170)

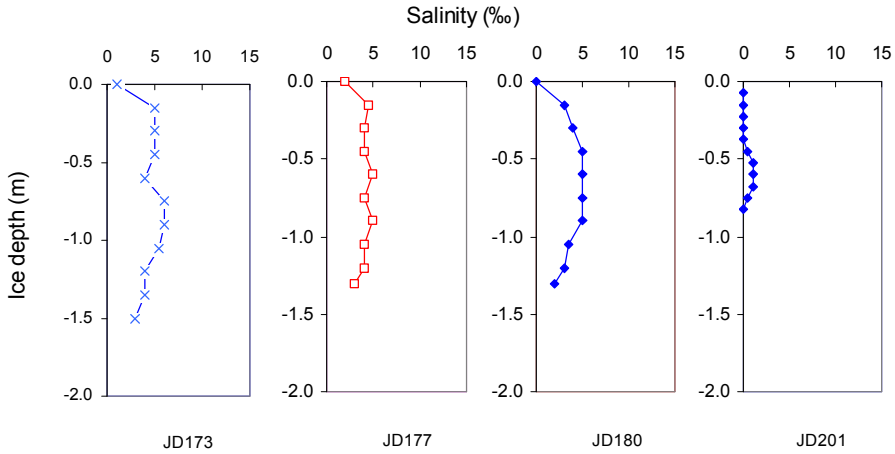

(b) 21 June (JD173) to 19 July (JD201)

Figure 8 Salinity profiles during the study

5. Borehole Strength

More than 100 borehole jack tests were conducted during the study. The borehole jack data from each test were used to generate three plots, (a) *in situ* ice pressure versus time, (b) indentor penetration (one half the displacement of the two end platens) versus time and (c) *in situ* ice pressure versus indentor penetration. Indentor penetration is defined as one-half the diametrical displacement of the borehole jack. Figure 9 is a schematic that shows the *in situ* pressure (s) and indentor penetration (d) as a function of time. The figure shows that, as the borehole jack is extended, the *in situ* ice pressure increases until it a peak pressure is attained, s_M. Typically, after s_M has been reached, the pressure drops and then stabilizes.

A standardized approach was needed to compare results from the 110 borehole jack tests. Since s_M was not always captured during the tests (due to the limit of the stroke ram and/or concern about overloading the jack), the common factor used to compare all tests was defined as s_{3mm}, the *in situ* pressure at an indentor penetration of 3 mm. Figure 9 shows a comparison between s_M and s_{3mm}. During the early borehole jack tests, the ice was sufficiently cold so that s_M occurred after a penetration of 3 mm (d_{3mm}). As the ice decayed, its temperature increased and the ice presented less resistance to the indentor. As a result, s_M was reached more quickly and there was very little (if any) difference between s_M and s_{3mm}, as discussed subsequently.

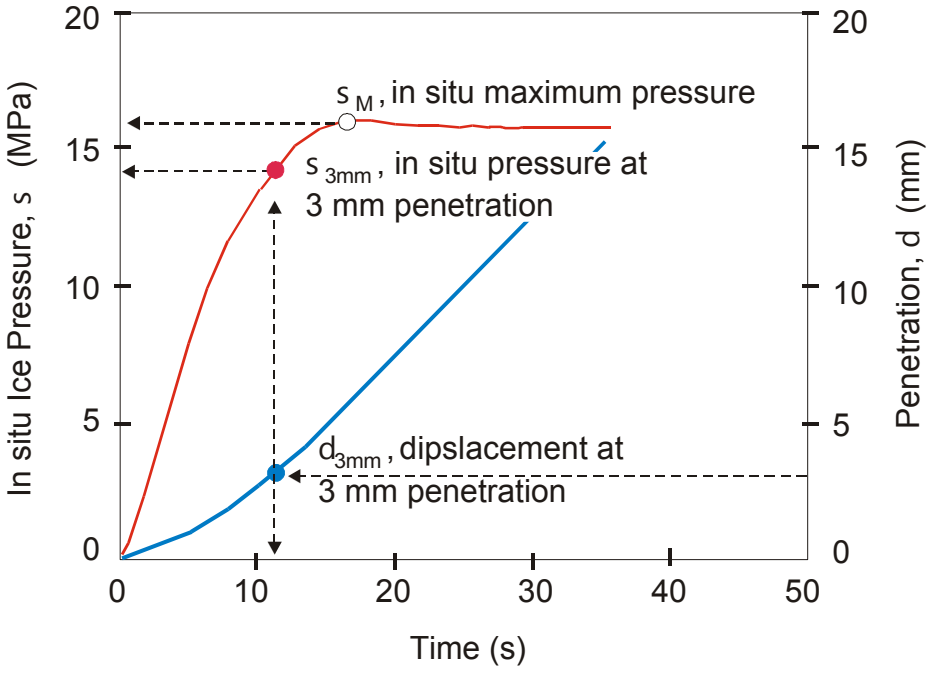

Figure 9 In situ pressure at 3 mm penetration and peak pressure for arbitrary test

Figure 10 shows the ice pressure (s) and indentor penetration (d) versus time curves for the surface layer of ice for two different borehole jack tests. First shown is the *in situ* borehole strength of cold ice at the beginning of the study (–7°C on 21 May, JD142). In comparison, Figure 10-b shows the *in situ* borehole strength of warm ice at the end of the study (–1.8°C on 19 July, JD201). The two borehole jack tests show that cold first year ice had a s_{3mm} of 14.8 MPa whereas warm, decayed ice had a s_{3mm} of only 1.9 MPa. The overall shape of the curves is considerably different for the two tests. Figure 10-a shows that the pressure continued to increase until the borehole jack was retracted at 19 s. Figure 10-b shows that the ice pressure reached a plateau after about 5 s, and remained at that level until the jack was retracted (at about 25 s).

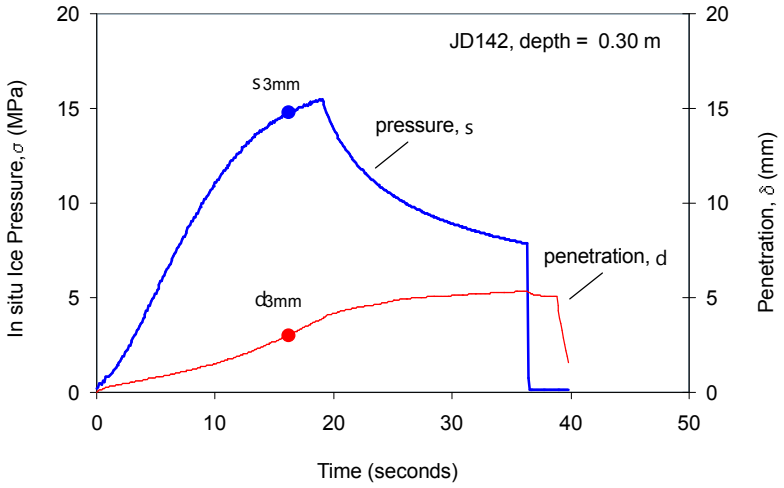

(a) 21 May (JD142)

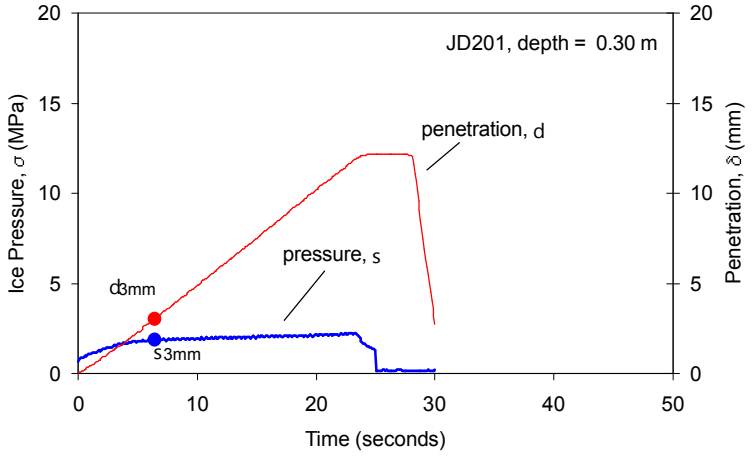

(b) 19 July (JD201)

Figure 10 Two examples of σ and δ in surface layer of ice, d = 0.30 m

5.1 Borehole Jack Data as a function of Ice Depth and Time

Figure 11 shows s_{3mm} for ice depths of 0.3 m, 0.6 m, 0.9 m and 1.2 m as a function of the day on which the tests were conducted. The plots include the borehole jack measurements from each hole (crossed data symbol) as well as the average of the individual *in situ* borehole strengths (oversized symbol).

5.1.1 Ice Depth 0.3 m

Figure 11-a shows that s_{3mm} decreased by about 1 MPa per week during the first four weeks (JD142 to JD163, 21 May to 11 June). A much larger decrease of 4.5 MPa in s_{3mm} occurred during the fourth week (JD163 to JD170, 11 June to 18 June). After that, there was a gradual reduction in s_{3mm} until the last tests were conducted on JD201 (19 July). Note that the strength of the surface layer changed only 0.6 MPa during the last three weeks of the study (JD183 to JD201, July 1 to July 19). Most of the change in ice strength at this depth occurred between the third and sixth weeks. The change in s_{3mm} that characterized the ice from JD156 to JD183 was used to calculate the average rate of ice decay (0.5 MPa/day). There was not much variation in s_{3mm} for the different tests that were conducted on the same day.

5.1.2 Ice Depth 0.6 m

Although the surface layer of ice began to decrease in strength during the first three weeks of the program, s_{3mm} at a depth of 0.60 m remained relatively unchanged (at 12 MPa, Figure 11-b). The most significant change in s_{3mm} occurred between JD156 (4 June) and JD163 (11 June). Within one week s_{3mm} had decreased by 4 MPa. The average rate of ice decay was 0.5 MPa/day from JD156 to JD183. The borehole strengths at a depth of 0.60 m did not deviate substantially for different tests conducted on the same day.

5.1.3 Depth 0.9 m

The ice at a depth of 0.90 m showed a very uniform decline in s_{3mm} until 1 July (JD183, Figure 11-c). At that point, s_{3mm} reached a plateau of about 3.5 MPa. One data point is used to show s_{3mm} at a depth of 0.90 m for 19 July (JD201). That is because by the end of the study the ice at only one of the boreholes was sufficiently thick to take a measurement at a depth of 0.90 m. The ice thickness was 0.95 m for that test. As such, the test was conducted 50 mm from the ice-water interface and would have been unreliable due to edge effects. The average rate of ice decay from JD156 to JD183 was 0.3 MPa/day. There was good agreement between s_{3mm} for individual borehole jack tests conducted on the same day.

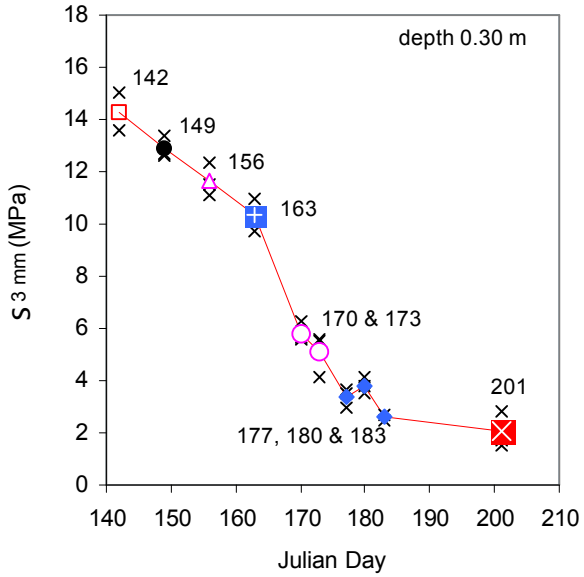

(a) depth 0.30 m

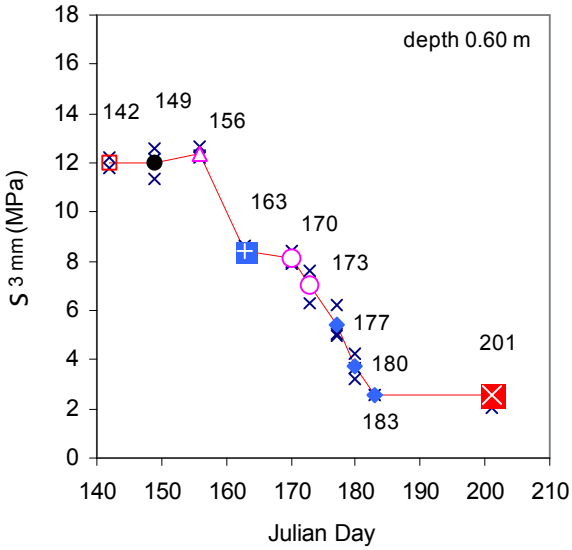

(b) depth 0.60 m

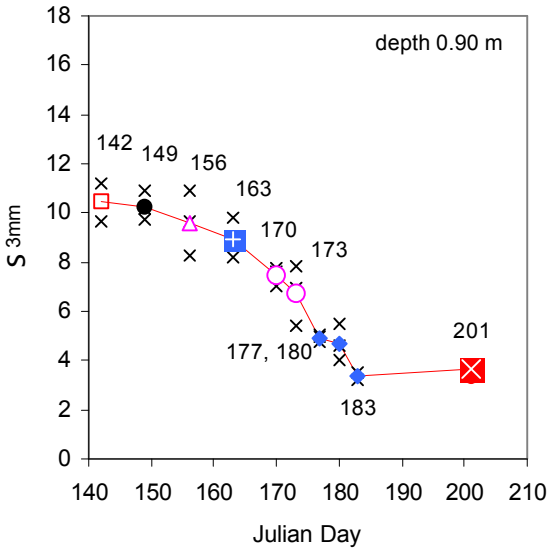

(c) depth 0.90 m

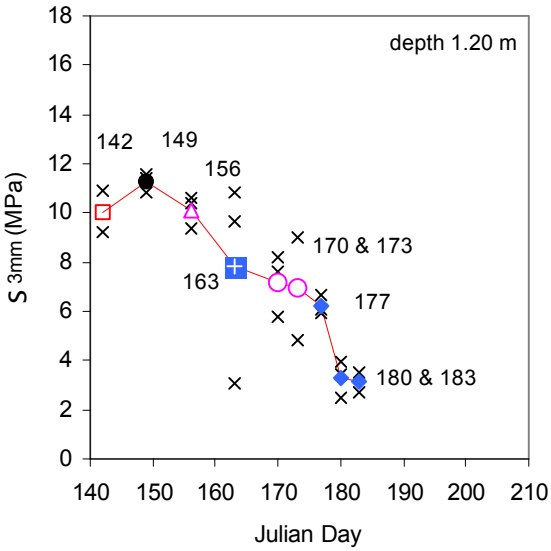

(d) depth 1.20 m

Figure 11 Seasonal changes in the *in situ* borehole strength, σ

5.1.4 Depth 1.20 m

Figure 11-d shows that, for the bottom ice, the most significant decrease in σ_{3mm} occurred from 25 to 28 June (JD 177 to JD180). Within the course of three days, σ_{3mm} had decreased by 3.0 MPa. The ice decay rate from JD156 to JD183 was 0.4 MPa/day. Unlike the borehole jack tests conducted at the other depths, tests from a depth of 1.2 m show considerable scatter in σ_{3mm} between 11 to 21 June (JD163 to JD173). Since only those tests showed scatter in σ_{3mm}, the variation was probably an artifact introduced during testing.

5.2 Influence of Stress Rate on Borehole Jack Measurements

It has been shown by Sinha (1997) that the *in situ* ice strength obtained from borehole jack tests is dependent upon stress rate, $\dot{\sigma}$. The rate effect was explored in this section to determine the contribution of stress rate ($\dot{\sigma}$) to the reduction in *in situ* ice strength (σ). Since the borehole jack used in this study did not have the option to specify stress rate, the stress rate for each test was determined by dividing σ_{3mm} the by the elapsed time.

Figure 12 is a compilation of the results of σ_{3mm} for all borehole jack tests conducted during the study. The results are categorized according to the day on which the test was conducted and the site at which the tests were conducted (main site or secondary sites sampled on 19/20 July). Superimposed on the borehole measurements is the stress rate ($\dot{\sigma}$) effect obtained by Sinha (1997), based upon the maximum *in situ* borehole stress (σ_M) of the surface layer of cold, first year sea ice (–7°C) for specified stress rates.

The comparison shows that, for similar stress rates, the borehole strengths measured during this study (σ_{3mm}) were less than those measured by Sinha (σ_M). For example, the highest σ_{3mm} measured during this study was 14.8 MPa on 21 May (JD142) in –7°C ice at a $\dot{\sigma}$ of 0.90 MPa/s. According to Sinha (1997), $\dot{\sigma}$ of 0.90 MPa/s would result in σ_M of 17.7 MPa for –7°C sea ice. The difference of 2.9 MPa between σ_M and σ_{3mm} for cold first year ice is to be expected, since this study relied upon *in situ* ice pressures at a specific penetration (σ_{3mm}) whereas the ice pressures reported by Sinha were the maximum ice pressure (σ_M). The different borehole jack assemblies and the different types of sea ice in the two studies would have also resulted in some variation.

Figure 12 shows a distinct difference in shape between the linear, stress rate effect reported by Sinha (1997) and the borehole jack data from this study. The different trends show that rate effect accounts for a only a small portion of the 9 MPa decrease in σ_{3mm} that occurred from 21 May (JD142) to 19 July (JD201). Rate effect would account for about 2 MPa of the decrease in σ_{3mm} between JD142 and JD201 (difference in average stress rate of 0.4 MPa/s). Most of the reduction in σ_{3mm} resulted from changes in ice properties such as temperature, salinity and density.

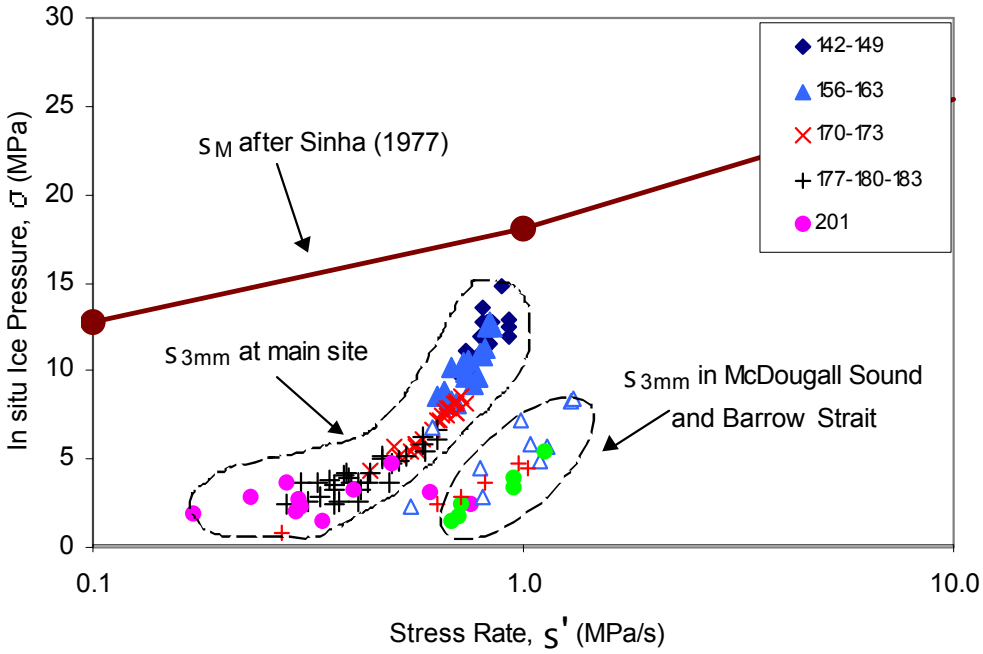

Figure 12 Effect of stress rate (σ') on ice borehole strength (σ)

6. Relation between Physical Properties and Borehole Strength

Figure 13 illustrates the relation between the average *in situ* borehole strength ($\underline{s}_{3mm}$) (averaged over the full thickness of the ice) and changes in physical properties of the ice. The warm air/ice temperatures after 28 June (JD180) made it difficult to accurately measure the ice salinity due to accelerated brine drainage. However the late-season salinity measurements do show that the ice became nearly fresh during the late stages of ice decay. Ice temperature measurements after 11 June (JD163) are subject to uncertainty, for previously discussed reasons.

The first notable decrease in $\underline{s}_{3mm}$ occurred between JD156 and JD163. The *in situ* ice strength, $\underline{s}_{3mm}$, was 11 MPa on 4 June (JD156) and had decreased to 9 MPa by 11 June (JD163). The decrease in $\underline{s}_{3mm}$ continued until 1 July (JD183), when the ice reached a plateau of 3 MPa. The *in situ* ice strength remained at the 3 MPa plateau until the last measurement was taken on 19 July (JD201).

Although $\underline{s}_{3mm}$ began to decrease on 4 June (JD156), the ice thickness did not change appreciably (from 1.5 m) until two weeks later (18 June, JD170). Between 18 June (JD170) and 19 July (JD201) the ice thickness decreased by 0.67 m. Ice ablation continued until the end of the study; three weeks after $\underline{s}_{3mm}$ reached a plateau. Despite the different intervals over which $\underline{s}_{3mm}$ and the ice thickness decreased, both occurred at uniform rates. The rate of decrease of $\underline{s}_{3mm}$ was 0.30 MPa/day (until 1 July, JD180) and the ice thickness decreased by 23 mm/day (until the last measurement was obtained on 19 July, JD201).

What were the external factors that resulted in first, a decrease in ice strength and second, a decrease in ice thickness? Figure 13 shows that the air temperature and ice temperature obviously influenced the onset of ice decay. On 10 June (JD162) the mean air temperatures rose above zero for the first time that season and the snow cover rapidly melted. The first signs of decreased ice strength coincided with the decrease in snow cover and increase in air/ice temperatures. After the insulating layer of snow melted, the ice was exposed to the warm air temperatures and the ice rapidly desalinated and began to ablate. The ice strength continued to decrease until it reached a plateau. The stabilization in ice strength coincided with the point at which the ice had desalinated almost completely.

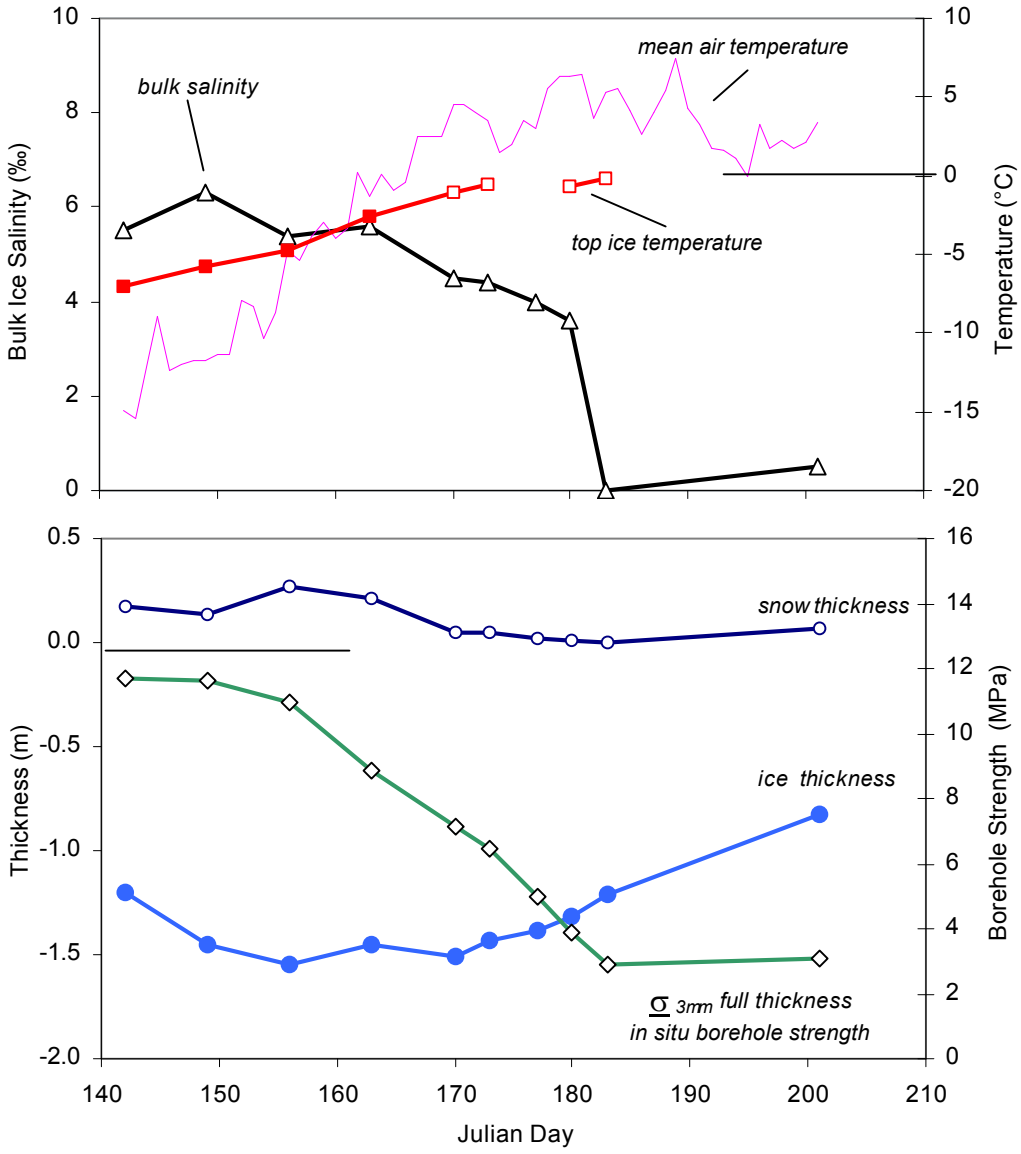

Figure 13 Relation between physical property measurements and $\underline{\sigma}_{3mm}$

7. Comparison of Measured and Calculated Ice Strengths

When a ship transits ice, the ice most frequently fails in bending. Frequently, flexural failure of the ice (s_f) is accompanied by ice crushing, resulting in a combined failure mode. The flexural strength of the ice (s_f) is most applicable to bending and the uni-axial compressive strength of the ice (s_c) is most relevant to ice crushing. Flexural and compressive strengths of the ice are essential for determining the loads applied to offshore structures and are also applicable to bearing capacity problems.

7.1 Calculation of the Unconfined Compressive Strength of the Ice

Many investigators (Wang, 1979; Frederking and Timco, 1980 and Sinha, 1981 to name a few), have measured the uni-axial compressive strength (s_c) of small samples of ice. Since measurements of s_c can be labor intensive and frequently are wrought with difficulty, Timco and Frederking (1990) developed an empirical model for calculating s_c for first year sea ice. Their model relies upon ice salinity, ice temperature, ice density and strain rate (Figure 1). Using their approach, the ice sheet is divided into nine layers. The total porosity (combined brine and air volume) of each layer is calculated from the ice temperature, salinity and density. The s_c of each of the nine layers of ice is calculated using equations that were developed from small-scale test data. The bulk compressive strength of the ice cover, $\underline{s}_c$, is the average strength of the nine layers.

7.2 Calculation of the Flexural Strength of the Ice

Timco and O'Brien (1994) compiled existing data on the measured flexural strength of the ice (s_f). Based upon the data, they formulated an empirical relation between s_f and the brine volume (n_b). The brine volume can be determined using ice temperature and salinity measurements (Frankenstein and Garner, 1967). It can also be determined (more accurately) using the equation given by Cox and Weeks (1982) which relies upon the measured density, temperature and salinity of the ice. The s_f can be determined from Equation 1 (after Timco and O'Brien, 1994).

$$\sigma_f = 1.76\, e^{-5.88\sqrt{\upsilon_b}} \qquad (1)$$

where
s_f = flexural strength of the ice
n_b = brine volume

7.3 Strength Comparison

Figure 14 shows the relation between measurements obtained from the borehole jack (average *in situ* confined compressive strength of the ice, $\underline{s}_{3mm}$) and the calculated flexural strength (s_f) and the calculated, averaged unconfined compressive strength ($\underline{s}_c$) of the ice. The measured top ice temperature and ice salinity and the calculated brine volume and total porosity are also shown in Figure 14. The calculated flexural strength (s_f) is a function of the brine volume (n_b) and the calculated unconfined compressive strength (s_c) is a function of the total porosity (n_t). The total porosity (n_t) was calculated for a constant ice density of 0.92 Mg/m³. An assumed ice density was used because the rough approximations of ice density obtained from ice freeboard measurements made during the field program produced invalid data and irregular trends. Strain rate ($\dot{e}$ in s^{-1}) was the second input parameter that was required to calculate s_c. Rather than the strain rate, the normalized indentor penetration rate ($\dot{d}$) of 0.002 s^{-1} was used, since it is more appropriate for the comparison. Although $\dot{d}$ of 0.002 s^{-1} was used for the comparison, equations for calculating s_c were based upon an upper limit for $\dot{e}$ of 0.0001 s^{-1}.

Figure 14 shows that $\underline{s}_{3mm}$ is roughly four times $\underline{s}_c$ (for $\dot{d}$ of 0.002 s^{-1}) and an order of magnitude larger than s_f. The three different strengths all decrease as the decay season progressed. Results showed, that once the air and ice temperatures increase, it is especially difficult to obtain reliable measurements of the ice temperature, salinity, and especially the density; parameters that are required to calculate the ice strength. Since the equations to calculate the flexural strength (s_f) and unconfined compressive strength (s_c) are so strongly dependent upon the physical properties of the ice, calculations were not reported after 21 June (JD173); the point after which the physical property measurements became unreliable.

The equations that provide reliable estimates of the strength of cold sea ice break down when the ice temperatures are with several degrees of the melting point of ice. Measuring the *in situ* strength of the ice with the borehole jack assembly circumvents problems associated with physical property measurements of decaying ice. The instrument proved extremely effective in providing quantitative evidence of the decrease in ice strength during the decay process; evidence that was shown to parallel trends in s_f and s_c.

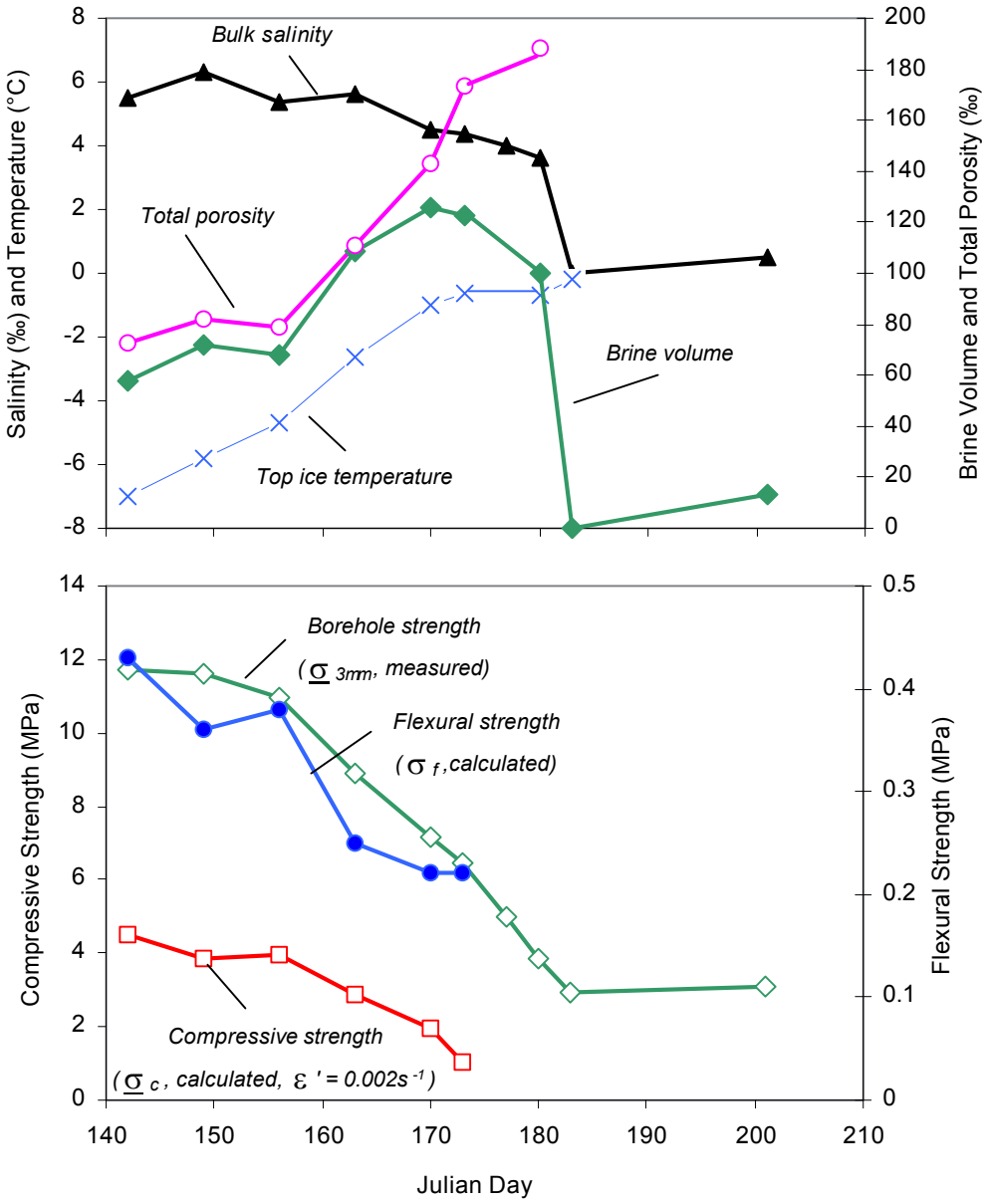

Figure 14 Comparison of $\underline{\sigma}_{3mm}$, σ_f and σ_c

8. Conclusions

The nine-week study was conducted from 21 May to 19 July 2000. Surface property measurements included the air temperature, snow depth and snow density. The measured bulk physical properties of the ice included freeboard, thickness, temperature, salinity and *in situ* confined compressive strength of the ice. A cursory examination of the relation between the measured surface properties and the bulk physical properties was made. Such a correlation would enable the mechanical strength of decayed ice to be included in the stages of ablation discussed in Barber (1997).

Mean air temperatures increased steadily during the study from –15°C to a maximum of +7.5°C, near the end of the study. Physical property measurements began on 21 May at which time the ice thickness was 1.20 m. The ice continued to increase in thickness until 4 June, when a maximum thickness of 1.55 m was attained. The ice remained about 1.5 m thick until two weeks later, 18 June, when it began to ablate. As ablation continued, the ice developed an undulating surface. When the last measurements were conducted on 19 July the ice was only 0.83 m thick. The 0.67 m of ice that ablated during the study did so at a relatively constant rate of 23 mm/day.

Salinity measurements showed that the surface and underside of the ice began to desalinate at about the same time. During the decay process, the ice developed a salinity profile distinctly different from the “C” shaped profile that typically characterizes cold, first year sea ice (higher salinity in the upper and lower parts of the ice sheet, see Nakawo and Sinha, 1981). Rather, the upper and lower surfaces of the ice began to desalinate before the bulk layer of ice, causing a reversed “C” shaped salinity profile. The ice maintained a reversed “C” shaped profile until the last salinity measurements were made on 19 July, at which point entire ice thickness was nearly devoid of brine (ice salinity of 0.5 ‰).

The *in situ* confined compressive strength of the ice (σ) was measured in 110 borehole jack tests. Once (or twice) per week, the tests were conducted in a number of boreholes, at depth intervals of 0.30 m. Typically, four borehole jack tests were performed in each hole. There was good repeatability of the data; measurements show that tests conducted on the same day had little variation in the σ when sampled at the same depth. All strength profiles showed that σ decreased as the decay season progressed.

The borehole strengths from each test were compared using 3 mm indentor penetration as a common factor (σ_{3mm}). During the first three weeks of the study, σ_{3mm} in the surface layer of ice (depth 0.30 m) was about 2 to 4 MPa higher than in the bottom layer of ice. By 18 June, however, the ice surface had deteriorated to such an extent

that s_{3mm} in the bottom ice was larger than near the ice surface. After 25 June s_{3mm} of the upper and lower ice surfaces were quite similar.

Over the nine-week period, the average full-thickness strength of the ice ($\underline{s}_{3mm}$ obtained by depth-averaging individual borehole strengths) decreased from 12 MPa to 3 MPa. Most of the decrease in $\underline{s}_{3mm}$ resulted from changes in the physical properties of the ice. About 20% (2 MPa) of the decrease was caused by the different stress rates of the borehole jack tests. The first significant decrease in $\underline{s}_{3mm}$ (2 MPa) occurred from 4 to 11 June. The $\underline{s}_{3mm}$ decreased by a relatively constant rate of about 0.30 MPa/day until 1 July when it reached 3 MPa. Once $\underline{s}_{3mm}$ had decreased to 3 MPa, it remained at that level until the end of the study (three weeks later). Results showed that while the ice started to ablate nearly two weeks after the ice strength began to decrease, ice ablation continued until the end of the study (three weeks after $\underline{s}_{3mm}$ had reached the 3 MPa plateau).

Comparison of the measured and calculated ice strengths indicated that the unconfined compressive strength of the ice (s_c) was about one-fourth of the *in situ* borehole strength ($\underline{s}_{3mm}$) whereas the flexural strength (s_f) was an order of magnitude less than s_{3mm}. The equations provided an estimate of ice strength up to a certain point; after that the equations were limited by unreliable physical property measurements of the ice. Since the borehole jack assembly provided *in situ* measurements of the ice strength, it was independent of physical property measurements and proved especially useful for late-season measurements.

9. Recommendations

This report was a first attempt to establish a relation between the surface properties, bulk properties and the mechanical strength of the ice throughout the decay process. That relation was a necessary step in order for a more rigorous form of ice decay to be incorporated into the Arctic Ice Regime Shipping System (AIRSS). Realizing that more data are needed before this can be achieved, a second season of decayed ice measurements has been scheduled for Spring, 2001. The data obtained during spring 2000 (and planned for spring 2001) provide a record of the ice decay process that extends later than any data presently available. Data collection on decayed ice will fulfill part of the objective, however, there must be adequate analysis of the measurements once they have been obtained. A basis must be developed for adjusting the AIRSS Multipliers for ice decay and for relating the modified Ice Multipliers to the Stages of Ablation. Only then may the understanding of the ice decay process be used successfully to adjust the AIRSS Ice Multipliers.

10. Acknowledgments

Transport Canada provided financial support for this project. Field measurements were undertaken by R. DeAbreu, K. Asmus, K. Wilson and D. Bradley of Canadian Ice Service. Field support from the University of Manitoba personnel and Polar Continental Shelf Project is also gratefully acknowledged. Greatly appreciated is the support of Canadian Coast Guard in providing the Louis S. St. Laurent as a working platform from which to access first year sea ice in its advanced stages of decay.

11. References

Barber, D (1997) Sea Ice Decay: Phase I. Centre for Earth Observation Science, University of Manitoba, Winnipeg, Canada, March 1997, 108 pp.

Cox, G. and Weeks, W. (1974) “Salinity Variations in Sea Ice”. J. Glaciol. 13 (67), pp. 109 – 120.

Frankenstein, G.E. and Garner R. (1967) “Equations for Determining the Brine Volume of Sea Ice from –0.5 to –22.9°C”. J. Glaciol. 6 (48), pp. 943 – 944.

Frederking, R. and Timco, G. (1980) NRC Ice Property Measurements during the Canmar Kigroriak Trials in the Beaufort Sea, winter 1979 – 80. DBR Pap. 947, DBR/NRC Rep., Ottawa, Ontario.

Frederking, R.M.W. (2000) Testing the Compressive Strength of Sea Ice with a Borehole Jack: Field Instructions. Report submitted to Canadian Ice Service by Canadian Hydraulics Centre of the National Research Council of Canada, April 2000, Technical Report HYD-TR-055, Ottawa, Ontario.

Johnston, M. and R.M.W. Frederking (2000) Seasonal Decay of First Year Ice: Field Measurements. Report submitted to Transport Canada and Canadian Ice Service by Canadian Hydraulics Centre, HYD-TR-057, Ottawa, Ontario, 21 pp.

Nakawo, M. and N.K. Sinha (1981) "Growth Rate and Salinity Profile of First Year Sea Ice in the High Arctic", J. Glac., Vol. 27, No. 96, pp. 315 – 330.

Masterson, D.M., Graham, W.P., Jones, S.J. and G.R. Childs (1997) "A Comparison of Uniaxial and Borehole Jack Tests at Fort Providence Ice Crossing, 1995", Can. Geotech. J., Vol. 34, pp. 471 – 475.

Prowse, T.D, Demuth, M.N. and C.R. Onclin (1988) "Using the Borehole Jack to Determine Changes in River Ice Strength", Proc. of Workshop on Hydraulics of River Ice/Ice Jams, Winnepeg, June 1988, pp. 283 – 301.

Sinha, N.K. (1981) "Rate Sensitivity of Compressive Strength of Columnar Grained Ice". Exper. Mech., 21 (6), pp. 209 – 218.

Sinha, N.K. (1986) "The Borehole Jack, Is It a Useful Arctic Tool?", Proc. Fifth Int. Offshore Mech. and Arctic Eng. Sym. (OMAE'86), Tokyo, Japan, 13 – 17 April, 1986, Vol. IV, pp. 328 - 335.

Sinha, N.K. (1990) "Ice Cover Strength Decay using Borehole Indentor", Proc. Tenth Int. Sym. on Ice (IAHR), Espoo, Finland, Vol. 2, pp. 735 – 744.

Sinha, N.K. (1997) "Borehole *In Situ* Indentation Tests in Floating Sea Ice at High Temperatures (> 0.97 T_m)". Proc. Ninth Int. Con. on Fracture (ICF9), 1 – 5 April 1997, Syndey, Australia, 8 pp.

Timco, G.W. and R.M.W. Frederking (1990) "Compressive Strength of Sea Ice Sheets". Cold Regions Science and Technology, Vol. 17, pp. 227 – 240.

Timco, G.W. and S. O'Brien (1994) "Flexural Strength Equation for Sea Ice". Cold Regions Science and Technology, Vol., 22, pp. 285 – 298.

Timco, G.W. and R.M.W. Frederking (1996) "A Review of Sea Ice Density". Cold Regions Science and Technology, Vol., 24, pp. 1 – 6.

Wang, Y.S. (1979) "Crystallographic Studies and Strength Tests of Field Ice in the Alaskan Beaufort Sea". Proc. POAC 79, Trondheim, Norway, Vol I., pp. 651 – 665.